Interaction between deformed nuclei at finite temperature

M. Rashdan
Department of Mathematics and Theoretical Physics, Atomic Energy Authority, Cairo, Egypt
(Received 15 December 1995; revised manuscript received 20 March 1997)

Within a complex free-energy density functional, derived from a realistic nucleon-nucleon interaction, the dependence on temperature of the real and imaginary parts of the free interaction energy of the deformed system U-U is investigated. It is found that the potentials strongly depend on orientations and temperature, where at zero orientation angle ($\beta=0°$) the potentials acquire repulsion, with increasing temperature, up to a critical value ($T\sim 3$ MeV), where shell effects become very small; beyond this value the potentials inverse this behavior. For large values of β the potentials become more and more attractive with increasing temperature. At much higher excitation ($T\sim 5$ MeV) the potentials become insensitive to orientations, due to the disappearance of shell corrections. The dependence of the relative momentum per nucleon on the internuclear distance is also investigated. [S0556-2813(97)05208-4]

PACS number(s): 25.70.Jj, 21.10.Gv, 24.10.Pa, 25.70.Lm

I. INTRODUCTION

The deformation degrees of freedom play an important role in deep inelastic scattering as well as in fusion reactions [1–6]. The deformation of fragments was phenomenologically studied by different groups. For example, Siwek-Wilczynska and Wilcznski [1] showed that the distribution of the final total kinetic energy versus the scattering angle depends strongly on the deformation degrees of freedom in deep inelastic collisions. They modified the potential in the exit channel due to deformations.

Schmidt, Toreev, and Wolschin and Froebrich, Strack, and Durand [3] have investigated the reaction between deformed nuclei through classical transport theory based on the solution of the Fokker-Planck equation. But, as indicated by Froebrich, Strack, and Durand [3], many effects such as quantal effects, deformations, and neck formations need to be included in their models. Indeed, the interactions (nuclear and Coulomb) that have been used in those calculations (e.g., in the determination of the friction forces and in the classical transport equations) have to be modified to be depend on orientations.

Muenchow and Scheid [4] have introduced a classical model with frictional forces to investigate deep inelastic scattering of deformed nuclei. The model has been applied to the heavy system U-U. The effect of temperature on the quadrupole deformation of the U nucleus has been considered. The interaction potential, which has been considered in those calculations, has been calculated (only at zero temperature) in the framework of the double-folding model, where a simple phenomenological two-body effective interaction of Gaussian type has been used. Although the model generally has reproduced the cross sections for deep inelastic scattering, a great difficulty to reproduce the large-energy losses observed in the double differential cross section has been found. This has been interpreted [4] to be due to the neck degree of freedom, which can be simulated with an internuclear potential in the exit channel. The potential in the exit channel should depend on temperature. Thus these applications [3,4] indicate the need for an accurate determination of the interaction between deformed nuclei that depends on orientations and temperature. This interaction can be used in both classical and quantum theories to describe the reactions of deformed nuclei.

The interaction potential between deformed nuclei has been calculated by many authors [2,6,7]. For example, in a previous work [6] we have calculated the optical potential between deformed nuclei, but at zero temperature, where it has been found that the potential strongly depends on deformations. We have also calculated the potential at finite temperature but between spherical nuclei [8]. Thus it is important to extend this later work [8] to the case of deformed nuclei. The temperature is expected to affect the interaction strongly because in deep inelastic scattering the nuclei are heated up during the reaction and might greatly change their initial configuration. Furthermore, the deformation of the nucleus decreases with increasing temperature, due to the decreases in shell effects, which are also expected to affect the interactions between deformed nuclei strongly.

In this work we consider the collision between two ^{238}U nuclei at finite temperature and we use the hot Breuckner G-matrix approach [8,9]. In this approach the kinetic- and potential-energy densities and the entropy density of the combined system are calculated in the momentum space configuration of two colliding nuclear entities separated by the relative momentum per nucleon K_r [9]. This approach for calculating the heavy-ion interactions is important since it is derived from the solution of the many-body problem in the framework of Brueckner theory, using a realistic nucleon-nucleon interaction, which is taken to be the Reid potential. Indeed, the collision dynamics (in each volume element in space) is approximated as a collision between two nuclear entities described by two Fermi spheres in momentum space. This is more appropriate for heavy-ion collisions than the single-nuclear-entity picture used by many authors. Furthermore, it is a density- and energy-dependent approach and thus it can be used to describe any colliding system where the inputs are the incident energy and the density distribution of the colliding nuclei.

The dependence of K_r on the real potentials and on the excitation energy, at each separation distance between the colliding nuclei, is investigated in detail. This was not con-

sidered in Refs. [8,9]. Section II presents the theoretical description. The calculations are presented and discussed in Sec. III.

It is obvious that initially the two nuclei have temperature zero because they are in their ground state. During the collisions they get excited and increase in temperature. The dynamical process of the excitation goes beyond the optical potential as in the case of the transfer reaction. Similarly, one would use in a deep inelastic scattering in the entrance channel the zero-temperature optical potential and in the exit channel a potential for a finite temperature as calculated here. The excitation mechanism is beyond the optical potential as in the transfer mechanism.

It is also worth noting that theoretical information on finite-temperature nuclei usually stems from a description of the nucleus either as a nuclear liquid in equilibrium with its vapor or as a heated finite metastable system in the vacuum. For temperatures below about one-half of the Maxwell critical temperature the thermostatic properties of nuclear systems derived from these two descriptions, however, do not differ much [10–12]. Since we are mainly interested in this work with low-energy nuclear collisions, where the temperature in the exit channel is expected to be small, one can use the thermodynamic relations. This approximation is widely adopted in the calculations of the interaction potential at finite temperatures [5,10,13,9].

II. THEORETICAL DESCRIPTION

As in Refs. [5,9,10,13], the interaction potential (free interaction energy) between two colliding nuclei separated by a distance R is defined at finite temperature T by the difference between the free energy of the combined system calculated at R and T and that calculated at infinity and T, i.e.,

$$V_F(K_r;R;T)=F(K_r;R;T)-F(K_r;\infty;T), \tag{1}$$

where K_r is the relative momentum per nucleon given at infinite separation by

$$K_r(R)\equiv K_r(\infty)=\sqrt{\frac{2m}{\hbar^2}\frac{E_{\rm lab}}{A_P}}. \tag{2}$$

Here m is the nucleon mass and A_P is the projectile mass. The free energy of the system F is obtained from the complex energy E and the entropy S as

$$F(K_r;R;T)=E(K_r;R;T)-TS(K_r;R;T), \tag{3}$$

where the entropy $S(K_r;R;T)$ of the system is obtained from the entropy density $s(\rho_P,\rho_T;R;K_r;T)$ through

$$S(K_r;R;T)=\int \frac{d^3k}{(2\pi)^3}\, s(\rho_P,\rho_T;R;K_r;T), \tag{4}$$

where

$$s=-g\int \frac{d^3k}{(2\pi)^3}\{n(\mathbf{k},T)\ln[n(\mathbf{k},T)] +[1-n(\mathbf{k},T)]\ln[1-n(\mathbf{k},T)]\}. \tag{5}$$

Here g is a spin-isospin degeneracy factor. For a system of two colliding nuclear matters in which one nuclear entity of density ρ_P with average momentum per nucleon K_r along the z axis in momentum space is colliding on another nuclear matter of density ρ_T at rest, the following form is assumed for the occupation probability n [9]:

$$n(\mathbf{k},T)=\begin{cases}\dfrac{1}{1+\exp\left(\dfrac{\hbar^2\mathbf{k}^2}{2mT}-\eta_T\right)} & \text{for } k_z\leqslant k_0\\[2ex] \dfrac{1}{1+\exp\left(\dfrac{\hbar^2(\mathbf{k}-\mathbf{K}_r)^2}{2mT}-\eta_P\right)} & \text{for } k_z>k_0,\end{cases} \tag{6}$$

where $k_0=[K_r^2+(2mT/\hbar^2)(\eta_P-\eta_T)]/2K_r$. The η's are determined by the normalization condition for the densities. In the definition (6) of the occupation probability the bare mass approximation is used. Obviously, in a more realistic situation one should use the effective mass instead of the bare mass in order to account for the momentum dependence of the single-particle (or the mean-field) potential in the nuclear medium [14]. However, this is important for intermediate- and high-energy nuclear collisions, where the density is high [14]. But for the case of direct nuclear reactions, the region of low-density overlap (the surface and tail regions of the potential) is the more important region. Thus one can use the bare mass approximation since the bare mass does not differ much from the effective mass at low density. Several authors used this approximation in their calculations of interaction potential at finite temperature [8,9,13,15,16].

The total energy of the system E is obtained from the complex energy density functional H through the relation

$$E(K_r;R;T)=\int d^3r\; H(r,R;K_r;T), \tag{7}$$

where

$$H(r,R;K_r;T)=\tau(\rho_P,\rho_T;K_r;T)+\Pi(\rho_P,\rho_T;K_r;T)+H_{\rm cor}. \tag{8}$$

The first term in Eq. (8) is the kinetic-energy density, which is calculated, in momentum space, from [9]

$$\tau(\rho_P,\rho_T;K_r;T)=\frac{\hbar^2}{2m}\left[g\int \frac{d^3k}{(2\pi)^3}\,k^2 n(\mathbf{k},T)\right]. \tag{9}$$

The second term in Eq. (8) is the complex potential-energy density $\Pi(\rho_P,\rho_T;K_r)$, which is calculated, at zero temperature, from the G matrix

$$\Pi(\rho_P,\rho_T;K_r)=\frac{1}{2}\sum_{\rm spin}\sum_{\rm isospin}\int_F \frac{d^3k}{(2\pi)^3} \times\int_F \frac{d^3k'}{(2\pi)^3}\,\langle kk'|G|kk'\rangle. \tag{10}$$

The reaction matrix G is the solution of the Bethe-Goldstone equation

$$G(W)=V+V\frac{Q}{W-H_0+i\epsilon}G(W), \tag{11}$$

where W is the starting energy and Q is the Pauli projection operator restricting the two nucleon intermediate states to be outside the Fermi sea. V denotes the bare nucleon-nucleon interaction taken to be the Reid soft-core potential. This equation is solved in momentum space for two colliding nuclear entities. The potential-energy density depends on temperature, indirectly, through its dependence on the hot nuclear densities. This is again a reasonable approximation at low temperature and it is widely used in most of the finite-temperature calculations [5,8,9,13,15,16]. The reason can be understand as follows: Finite nuclei disintegrate at temperatures around 6 MeV [4,16], which is smaller than the critical temperature of nuclear matter ($\sim 15-20$ MeV [17]), mainly due to surface effects. Thus one expects (at these small temperatures) that the contributions from the volume potential-energy part to the excitation energy is smaller than that which comes from the other parts (kinetic, surface, etc.). This has been predicted also for the case of a single nuclear matter, where the increases in the kinetic energy per particle with increasing temperature is larger than the increases in the potential energy per particle, especially at low densities and temperatures [18]. Thus one can neglect the modification of the potential-energy density due to temperature and simulate its temperature dependence through its dependence on the hot nuclear densities, at least at low temperatures, like that considered here ($\leqslant 5$ MeV).

It is worth noting that the free energy (which is the adequate potential for isothermal process), as defined through Eqs. (1)–(11), develops an imaginary part as a result of the microscopic treatment of the collisions between nuclei through the solution of the Bethe-Goldstone equation, even at zero temperature (as it has been done here) due to $2p$-$2h$ real excitations. The hot imaginary part is particularly important to get a reliable quantum-mechanical description of deep inelastic scattering. It is also important to describe the temperature dependence of the nucleon mean free path [19] and other, preequilibrium and equilibrium, finite-temperature absorption process [20].

The last term in Eq. (8) is a correction term due to surface and symmetry energies

$$H_{\rm cor}=\frac{\hbar^2}{8m}\chi(\nabla\rho)^2+D(\rho_n-\rho_p)^2\rho^\nu, \quad \nu=-\frac{1}{3}, \tag{12}$$

where χ and D are two parameters determined by minimizing the total binding energy of the ^{238}U nucleus with respect to the parameters of the density distribution in order to get good agreement for the binding energy and rms radius at zero temperature with the experimental values [16].

III. NUMERICAL CALCULATIONS AND DISCUSSION

The density distributions of ^{238}U is described by the deformed Fermi shape

$$\rho_{T,P}=\frac{\rho_0}{1+\exp\{[r-C(\theta)]/a\}}, \tag{13}$$

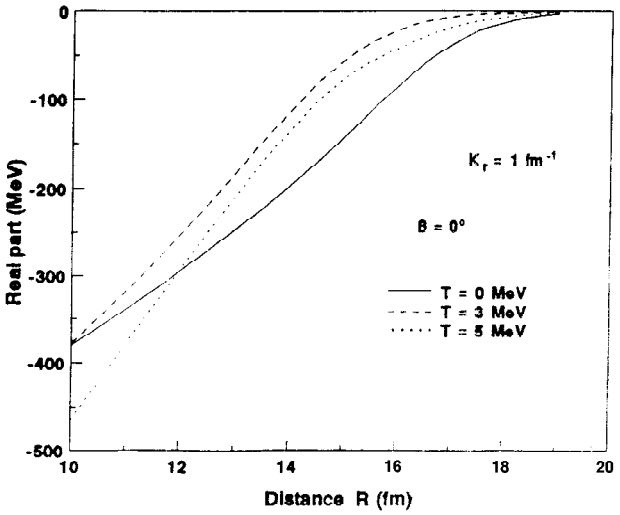

FIG. 1. Real part of the free interaction energy of the U-U system calculated against R at orientation angle $\beta=0°$, relative momentum per nucleon $K_r=1$ fm^{-1}, and $T=0$ (solid curve), 3 (dashed curve), and 5 (dotted curve) MeV.

where ρ_0 is the central density determined by normalization. $C(\theta)$ is given by

$$C(\theta)=C_0[1+\beta_2 Y_{20}(\theta)]. \tag{14}$$

The parameter C_0 is taken from electron scattering experiments [21] for the proton density distribution, while for the neutron density C_0 is increased by 0.2 fm more than that of the proton density [16].

The static deformation of the ^{238}U nucleus has its origin in shell effects. At high intrinsic excitation energies the shell effects vanish and the static deformation approaches zero [4,9,16,22]. This effect is simulated by taken the deformation parameter β_2 to be temperature dependent through the relation [4,16]

$$\beta_2(T)=\beta_2(0)e^{-T/T_0}, \tag{15}$$

where $\beta_2(0)=0.26$ and T_0 ($=1.5$ MeV [4]) is the temperature of the nucleus at which the shell effects start to vanish. This choice of the deformation parameter β_2 and its dependence on temperature is consistent with experiments at zero temperature [21] and is also compatible with the excitation energies predicted by our G-matrix calculations [16]. The diffuseness parameter a is determined by minimizing the total (nucleus plus Coulomb) free energy of the ^{238}U nucleus, at each temperature T, with respect to a [16].

Figure 1 shows the real part of the free interaction energy of the U-U system calculated against R at orientation angle $\beta=0°$, relative momentum per nucleon $K_r=1$ fm^{-1} and at temperature $T=0$ (solid curve), 3 (dashed curve), and 5 (dotted curve) MeV. The orientation angle β is the angle between the principal axes (which are taken to be parallel) and the line joining the two centers of masses of the nuclei. Figure 2 is the same as Fig. 1, but for the imaginary part. The total (real nuclear plus Coulomb) potential is shown in Fig. 3. The Coulomb potential is calculated using the double folding model of deformed nuclei [2]. The Coulomb potential depends on temperature through the hot nuclear densities.

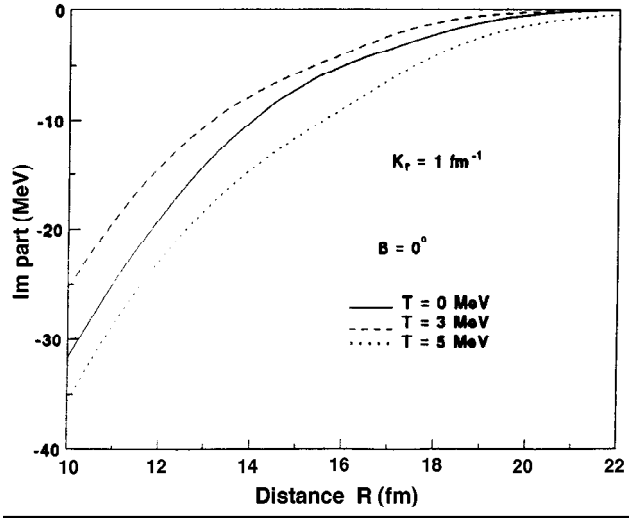

FIG. 2. Same as Fig. 1, but for the imaginary part.

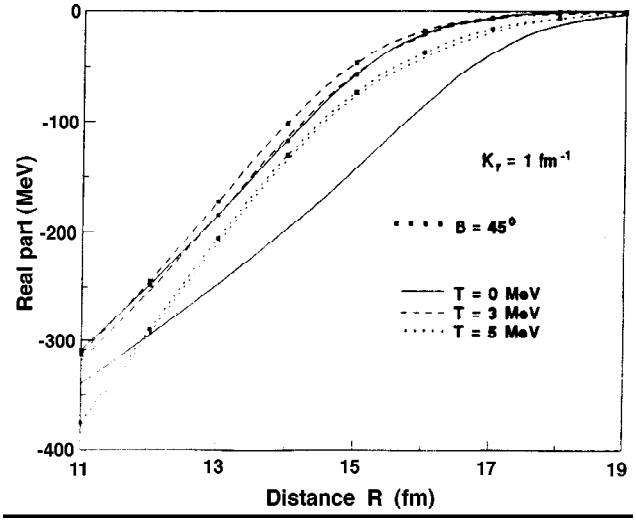

FIG. 4. Real part of the free interaction energy calculated at $\beta = 45°$ (curves with squares) in comparison with that calculated at $\beta = 0°$ (curves without squares).

As shown in Figs. 1 and 2 at $\beta = 0°$ by increasing the temperature both the real and imaginary parts of the interaction potential are repulsed up to temperature around 3 MeV, where shell effects nearly vanish and then the potentials are attracted with increasing temperature. The interaction barrier increases with increasing temperature up to $T \sim 3$ MeV; it decreases with increasing temperature, as shown in Fig. 3. This potential behavior at $\beta = 0°$ changes with increasing β. Figures 4 and 5 show the real and imaginary parts of the interaction potential calculated at $\beta = 45°$ (curves with squares) in comparison with that calculated at $\beta = 0°$ (curves without squares). Similar results for $\beta = 90°$ are shown in Figs. 6 and 7. As shown in these figures, at zero temperature, by increasing β the potential is repulsed due to the reduction in the overlap region. Increasing the temperature, the nuclei tend to the spherical shapes, due to the disappearance of shell effects, which decreases the deformations and thus reduces the overlap at $\beta = 0°$, but increases the overlap with increasing β. Thus, increasing the temperature reduces the repulsion occurring in the potentials with increasing β. At much higher excitations shell effects vanish and the nuclei nearly take the spherical shapes and thus the potentials become insensitive to orientations, as shown in Figs. 4–7, where $T = 5$ MeV the potentials calculated at different orientation angles are very close together.

The effect of the change in the relative momentum per nucleon at each separation due to the real potentials and the excitation energies is also investigated in this work. The calculations shown in Figs. 1–7 are carried out for a fixed value of K_r at all distances, where $K_r(R) \equiv K_r(\infty) = 1$ fm^{-1}. This value corresponds to the incident laboratory energy per nucleon, ~ 20.7 MeV. However, during the collisions $K_r(R)$ should be changed due to the attractive real nuclear potential $\mathrm{Re}(V_F)$, the repulsive Coulomb potential V_C, and the excitation energies. In order to consider these effects, $K_r(R)$ is calculated at each separation from

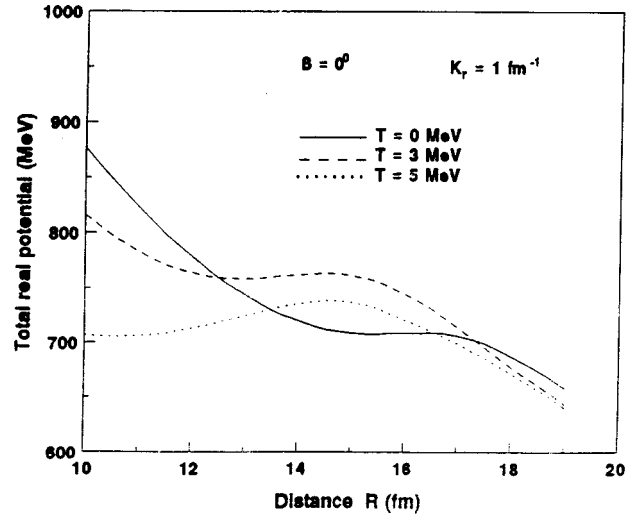

FIG. 3. Same as Fig. 1, but for the total (real nuclear plus Coulomb) potential.

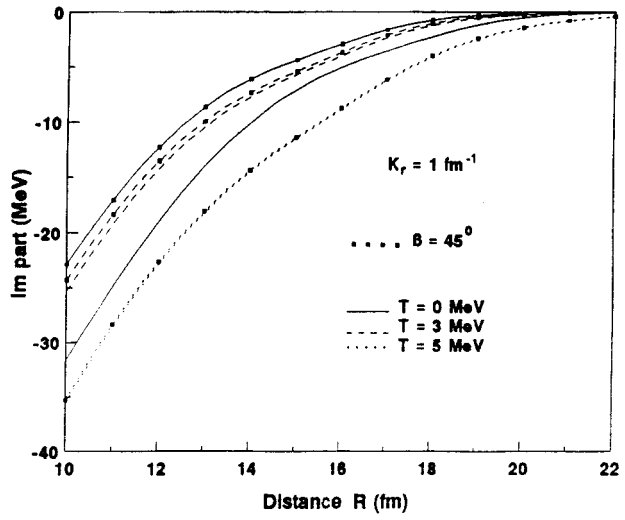

FIG. 5. Same as Fig. 4, but for the imaginary part.

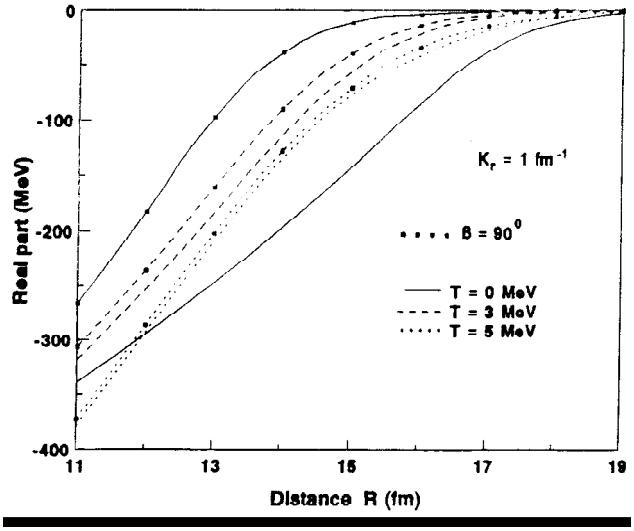

FIG. 6. Same as Fig. 4, but at $\beta=90°$.

$$\frac{\hbar^2}{2m}K_r^2(R)=\frac{\hbar^2}{2m}K_r^2(\infty)-2\frac{\mathrm{Re}[V_F(K_r(R);R;T)]}{A_P}-2\frac{V_C(R;T)}{A_P}-4\tilde{a}\,T^2. \tag{16}$$

A similar relation for the case of zero temperature is found in Ref. [7]. The level density parameter $\tilde{a}$ is taken to be 0.1 MeV^{-1} [16]. Although the energy-level density parameter depends, in principle, on the shell, pairing, and deformation effects as well as on the model used for the energy density, the value used here is already deduced from our previous G-matrix calculation [16] for the ^{238}U nucleus (see Table 2 in Ref. [16]). Moreover, this value of the energy-level density is, in general, consistent with other theoretical calculations and also with experiments [23–25].

Equation (16) is solved by iteration since the nuclear potential depends on $K_r(R)$. Figures 8, 9, and 10 show the real, imaginary, and total potentials, respectively, calculated at $\beta=0°$, and at $T=0$, and 3 MeV for relative momentum per nucleon determined from Eq. (16) (dashed curves) in comparison with that calculated with fixed $K_r(R)\equiv K_r(\infty)=1\ \mathrm{fm}^{-1}$ (solid curves). As shown in Figs. 8 and 9 the nuclear potentials calculated with nonfixed K_r [i.e., with $K_r(R)$ as determined from Eq. (16)] are less attractive in comparison to that calculated with fixed K_r (i.e., with $K_r=1\ \mathrm{fm}^{-1}$), especially in the surface region. At large separations the potentials calculated with nonfixed and with fixed K_r close together, as expected. The reason for the repulsion that occurs in the potentials calculated with nonfixed $K_r(R)$ (which increases when decreasing the internuclear distance R) is mainly due to the increase in the repulsive Coulomb potential, which overcomes the increase in the attractive nuclear potential and thus reduces the value of K_r. Obviously, the reduction in K_r presents less attractive nuclear potentials.

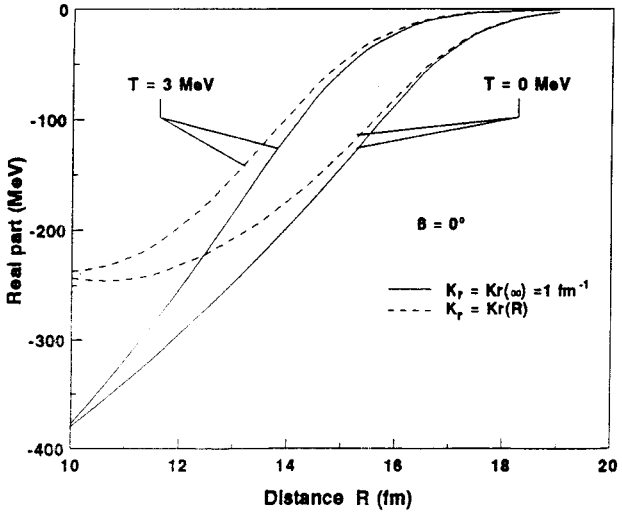

FIG. 8. Real part of the free interaction energy calculated at $\beta=0°$ and at $T=0$ and 3 MeV for the relative momentum per nucleon as calculated from Eq. (16) (dashed curves) in comparison with that calculated with fixed $K_r(R)=K_r(\infty)=1\ \mathrm{fm}^{-1}$ (solid curves).

In summary, we investigate the effect of temperature on the free interaction energy of the deformed U-U system. The

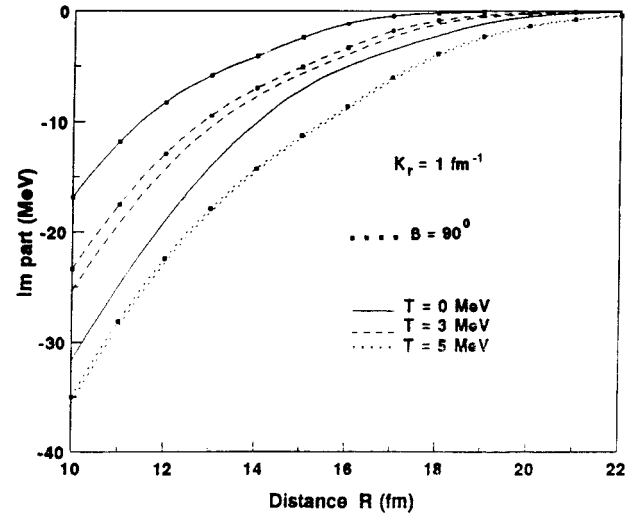

FIG. 7. Same as Fig. 5, but at $\beta=90°$.

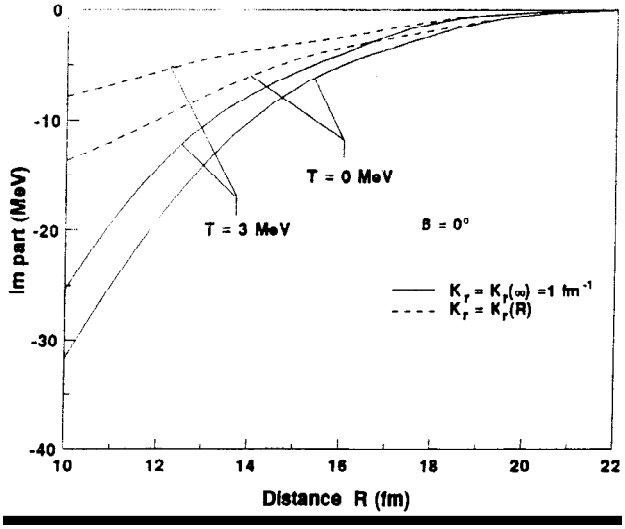

FIG. 9. Same as Fig. 8, but for the imaginary part.

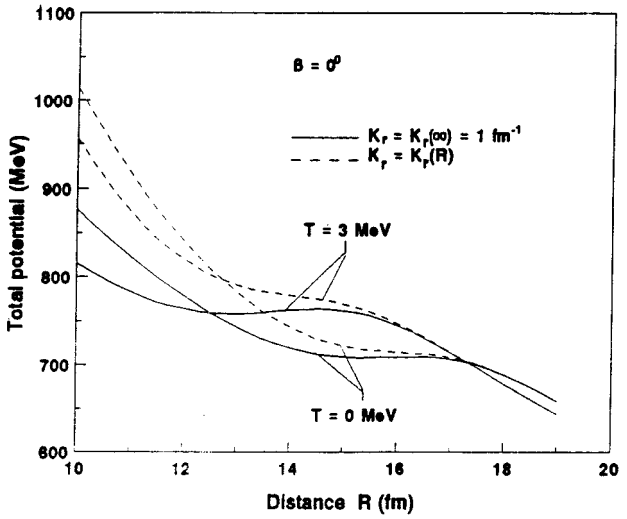

FIG. 10. Same as Fig. 8, but for the total potential.

free interaction energy is described in a realistic manner, where the entropy, kinetic-energy, and potential-energy densities of the composite system are calculated in the momentum space configuration of two colliding nuclear matters. In this procedure the free interaction energy depends on the bombarding energy. Furthermore, this approach yields an imaginary part of the interaction, which is important for the quantum-mechanical description of the inelastic processes. This is different from other calculations [5,10,13,15], in which the free interaction energy has been calculated within the single-nuclear-entity picture, which may not be appropriate for heavy-ion collisions.

It is also important to note that shell effects, which have been simulated in this work through the deformation parameters of the colliding nuclei, have been found to affect the interactions between deformed nuclei strongly. This is because the interactions strongly affected by deformations and orientations that strongly depend on shell effects. The dependence of the interactions on shell effects decreases with increasing temperature due to the decrease in the static deformation of the colliding nucleus. For much higher excitation ($T>5$ MeV) the nuclei become unstable and fragment into many particles. Finally, it is worth mentioning that the present interactions (real, imaginary, and total), which strongly depend on deformation, orientations, and temperature, are expected to be important in the investigations of the reactions between deformed nuclei.

ACKNOWLEDGMENTS

It is a pleasure to thank Professor W. Wadia and Professor M. Ismail for reading the paper and for fruitful discussions.

[1] K. Siwek-Wilczynska and J. Wilcznski, Nucl. Phys. **A264**, 115 (1976).
[2] M. J. Rhoades-Brown, V. E. Oberacker, M. Seiwert, and W. Greiner, Z. Phys. A **310**, 287 (1983).
[3] R. Schmidt, V. D. Toneev, and G. Wolschin, Nucl. Phys. **A311**, 247 (1978); P. Froebrich, B. Strack, and M. Durand, *ibid.* **406**, 557 (1983).
[4] M. Muenchow and W. Scheid, Phys. Lett. **162B**, 265 (1985); Nucl. Phys. **A468**, 59 (1987).
[5] D. Bandyopadhyay, S. K. Samaddar, R. Saha, and J. N. De, Nucl. Phys. **A539**, 370 (1992).
[6] M. Rashdan, A. Faessler, M. Ismail, and W. Wadia, Nucl. Phys. **A466**, 439 (1987); M. Rashdan, J. Phys. G **22**, 139 (1996).
[7] A. Faessler, M. Ismail, N. Ohtsuka, M. Rashdan, and W. Wadia, Z. Phys. A **326**, 437 (1987).
[8] M. Rashdan, A. Faessler, M. Ismail, and N. Ohtsuka, Nucl. Phys. **A468**, 168 (1987).
[9] A. Faessler, M. Rashdan, M. Ismail, N. Ohtsuka, and W. Wadia, Nucl. Phys. **A333**, 153 (1989).
[10] J. N. De and W. Stocker, Phys. Rev. C **42**, R819 (1990).
[11] W. Stocker, Phys. Lett. **142B**, 319 (1984).
[12] M. Brack, C. Guet, and H.-B. Hakansson, Phys. Rep. **123**, 267 (1985).
[13] U. Gaehde and W. Stocker, Nucl. Phys. **A278**, 117 (1977).
[14] D. T. Khoa, N. Ohtsuka, A. Faessler, M. A. Matin, S. W. Huang, E. Lehmann, and Y. Lotfy, Nucl. Phys. **A542**, 671 (1992).
[15] E. Tomasi, X. S. Chen, S. Leray, C. Ngo, M. Branco, X. Vinas, and H. Ngo, Nucl. Phys. **A389**, 69 (1982).
[16] M. Rashdan, A. Faessler, and W. Waida, J. Phys. G **17**, 1401 (1991).
[17] R. K. Su, S. D. Yang, and T. T. S. Kuo, Phys. Rev. C **35**, 1539 (1987).
[18] A. Faessler, M. Rashdan, and N. Ohtsuka (unpublished).
[19] A. H. Blin, R. W. Hasse, B. Hiller, and P. Schuk, Phys. Lett. **161B**, 211 (1985).
[20] M. Abe, S. Yoshide, and K. Sato, Phys. Rev. C **52**, 837 (1995).
[21] T. Cooper *et al.*, Phys. Rev. C **13**, 1083 (1976).
[22] A. S. Jensen and J. Damgaard, Nucl. Phys. **A203**, 578 (1973).
[23] M. Barranco and J. Treiner, Nucl. Phys. **A351**, 269 (1981).
[24] S. Song *et al.*, Phys. Lett. **130B**, 14 (1983).
[25] A. Chbihi *et al.*, Phys. Rev. C **43**, 666 (1991).